Thermochimica Acta 520 (2011) 99–104

Contents lists available at ScienceDirect

Thermochimica Acta

journal homepage: www.elsevier.com/locate/tca

Heat capacity for the binary system of silybin and poly(vinylpyrrolidone) K30

Yu-Li Li, Tong-Chun Bai*, Yan Yang

College of Chemistry, Chemical Engineering and Materials Science, Soochow University, Suzhou 215123, China

ARTICLE INFO

Article history:
Received 27 January 2011
Received in revised form 20 March 2011
Accepted 24 March 2011
Available online 5 April 2011

Keywords:
Silybin
Poly(vinylpyrrolidone) (PVP) K30
Heat capacity
DSC

ABSTRACT

The heat capacity C_p of solid mixtures of silybin and poly(vinylpyrrolidone) (PVP) K30 was measured by differential scanning calorimetry (DSC). The IUPAC name for PVP is 1-ethenylpyrrolidin-2-one, and that for silybin is 3,5,7-trihydroxy-2-[3-(4-hydroxy-3-methoxyphenyl)-2-hydroxymethyl-2,3-dihydrobenzo-[1,4]dioxin-6-yl]-chroman-4-one. By analyzing the curves of (dC_p/dT) against temperature T, some apparent points, a maxima point and a minima point, to characterize the C_p curve were obtained. The maxima point in the region of $w_1 < 0.4$ is a character of amorphous solid state of PVP, where w_1 is the mass fraction of silybin. In this region, silybin is dispersed into the amorphous solid of PVP. The minima point in the region of $w_1 > 0.4$ is a character of crystalline silybin. In this region, a mixture of crystalline silybin and an amorphous solid dispersion is observed.

1. Introduction

Silybin is an antihepatotoxic polyphenolic substance isolated from the milk thistle plant, *Silybum marianum*. Its structure is shown in Fig. 1. It is widely used as a drug to maintain liver health and to treat a range of liver and gallbladder disorders, including hepatitis, cirrhosis, and jaundice [1–3]. The poor solubility in water limits its biological and medicinal application. To improve the solubility and dissolution rate, a variety of methods have been developed, among them including methods to incorporate silybin in a dosage form using cyclodextrin complex, liposomes, and solid dispersions, respectively [4,5].

Solid dispersion is one of the most promising methods of improving the dissolution rate and bioavailability of poorly water-soluble drugs [6]. In these dispersions, the drug can be present in the fully crystalline, fully amorphous or partially crystalline and amorphous state. Often the amorphous solid dispersion of drug shows a greater solubility and dissolution rate in comparison to the crystalline material [7]. Some polymers such as poly(ethylene glycol) (PEG), poloxamer and poly(vinylpyrrolidone) (PVP) have been the common carriers used for solid dispersions [5,8,9]. Therefore, it is important to study a solid dispersion in pharmaceutical applications.

Poly(vinylpyrrolidone) (PVP), with the IUPAC name 1-ethenylpyrrolidin-2-one, is one of the most common compounds in making a solid dispersion drug [10–12]. Its amorphous solid state promotes the drug solubility and dissolution rate. During the preparation and medicinal application, the most important thing is to study the phase state of solid mixtures. To address this problem, the dependence of the phase state on the composition and the temperature must be known. Among many physical properties, heat capacity is an essential amount to study the phase transition, critical phenomena, and glass transition [13–17]. Therefore, basic data is important in evaluation of the efficiency of drugs.

In this work, solid dispersions and mixtures of silybin and PVP K30 were prepared by a solvent evaporation method. Heat capacity (C_p) of these binary systems was measured by differential scanning calorimetry (DSC). By analyzing the effect of composition on C_p, information about the phase state and the conditions to prepare a solid dispersion drug can be obtained.

2. Experimental

2.1. Materials

Silybin (CAS. no. 22888-70-6, with IUPAC name 3,5,7-trihydroxy-2-[3-(4-hydroxy-3-methoxyphenyl)-2-hydroxymethyl-2,3-dihydrobenzo-[1,4]dioxin-6-yl]-chroman-4-one) was purchased from Panjin Green Biological Development Co. Ltd., Liaoning, China. Its purity was 0.97 mass fraction determined by UV-spectrometry at (252–288) nm. This purity was confirmed by HPLC with 96.8% silybin, 1.1% isosilybin, 0.8% silydianin, 0.1% silychristin, and 1.2% other impurities. Poly(vinylpyrrolidone) (PVP) K30 (CAS. no.: 9003-39-8, with IUPAC name 1-ethenylpyrrolidin-2-one and a 0.985 mass fraction purity) was received from SinoPharm Chemical Reagents Co. Ltd. The main impurity in PVP is water. All samples were dried under vacuum at 333 K for 48 h before use.

* Corresponding author. Tel.: +86 512 65880363; fax: +86 512 65880089.
E-mail addresses: tcbai@suda.edu.cn, tcbai@sina.com (T.-C. Bai).

0040-6031/$ – see front matter © 2011 Elsevier B.V. All rights reserved.
doi:10.1016/j.tca.2011.03.022

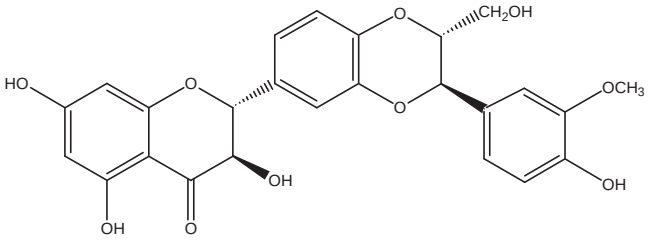

Fig. 1. Chemical structures of silybin. CAS: 22888-70-6. IUPAC name: 3,5,7-trihydroxy-2-[3-(4-hydroxy-3-methoxyphenyl)-2-hydroxymethyl-2,3-dihydrobenzo-[1,4]dioxin-6-yl]-chroman-4-one.

2.2. Preparation of samples

The pure samples of silybin and PVP were dried under vacuum at 333 K for 48 h to remove water. The freshly dried compounds were quickly weighed in a glass bottle with hermetic seal cover. Two accurately weighed compounds were mixed to form binary mixtures. The composition of the mixture is determined at this step. The mass fractions of silybin, w_1, in the mixtures used in this work are 0.1000, 0.1994, 0.2999, 0.3989, 0.5000, 0.5996, 0.6997, 0.8001 and 0.8996, respectively.

To prepare the sample to be a solid dispersion, liquid ethanol was added to dissolve the mixture. After sample dissolves in ethanol completely, the solvent was evaporated under reduced pressure at about 313 K in a rotary evaporator. After that, sample was dried under vacuum at 333 K over 48 h, and then it was stored over P_2O_5 in a desiccator before use. During this process, solvent was added and then removed, but the mass ratio of two components (silybin to PVP) is unchangeable. The initial value of composition is still an available choice.

2.3. DSC analysis and heat capacity measurements

The heat capacity was measured with a differential scanning calorimeter (NETSCH, DSC-204F1, Germany). Certified indium wire encapsulated in an aluminum crucible was used for temperature and heat flow calibration. An empty aluminum pan and lid was used as the reference for all measurements. Nitrogen gas with a purity of 0.99999 (volume fraction) was used as a purge gas at a rate of 20 mL min^{-1}, and protective gas was used at 70 mL min^{-1} in operation. Samples of about 5 mg were weighed to ±0.01 mg using a balance (model BT25S, Sartorius AG. Beijing). A thin disk of sapphire was used as the heat capacity standard.

The measurement of heat capacity includes three runs [14,15]. An empty Al pan with a lid was the first run to obtain the baseline. The second and third runs were performed on the sapphire and the sample, respectively. One empty Al pan was used through three runs. A three-segment heating program was used in DSC operation. The first segment lasting for 15 min was an isothermal one at the initial temperature; the second segment was a dynamic one with a heating rate of 5 K min^{-1}, and the final segment lasting for 15 min was another isothermal one at the final temperature. The heat capacity is calculated by Eq. (1).

$$C_{p,sam} = C_{p,std}\frac{(F_{sam} - F_{bsl})m_{std}}{(F_{std} - F_{bsl})m_{sam}} \quad (1)$$

where $C_{p,sam}$/J K^{-1} g^{-1} and $C_{p,std}$/J K^{-1} g^{-1} are the heat capacity of the sample and standard substance (sapphire), respectively. F_{sam}, F_{bsl} and F_{std} are the heat flows of the sample, baseline, and sapphire runs respectively, and m_{std} and m_{sam} are the masses of the standard substance and the sample, respectively.

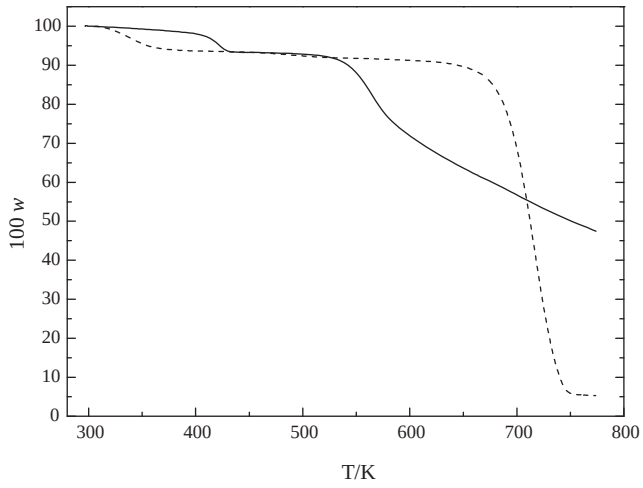

Fig. 2. The thermogravimetric trails (sample mass loss with temperature rising, w is mass fraction) of silybin (solid line) and PVP K30 (dash line).

2.4. Thermogravimetric analysis

Thermogravimetric (TG) analysis was used to determine the mass loss during the process of temperature programming. The TG experiment was performed with a TA Instruments SDT 2960 in a dynamic flow of nitrogen (0.99999 volume fraction). The gas flow rate was 100 mL min^{-1}. Approximately 2 mg of sample was weighed in an aluminum pan and heated from room temperature to 773 K at a rate of 10 K min^{-1}, and the loss of weight was recorded.

2.5. Infrared spectroscopy

Fourier transform infrared (FT-IR) spectra were obtained on a Magna 550 FT-IR system (Nicolet) with the KBr disk method. The scanning range was (400–4000) cm^{-1}, and the resolution was 2 cm^{-1}.

3. Results and discussions

3.1. Thermal analysis for pure PVP K30 and silybin

To set up the experimental steps and operation conditions to measure heat capacity, the thermal behavior of pure PVP and silybin was analyzed first.

The TG trails of silybin and PVP K30 are shown in Fig. 2. The mass loss due to water evaporation for silybin is found in the range from 406 to 420 K. Decomposition of silybin is found above 540 K. The TG trail of PVP K30 shows water evaporation below 393 K, and the temperature of molecule decomposition starts at 633 K. If sample was prepared carefully, the mass loss due to water evaporation can be reduced to less than 2%.

The DSC curve of silybin is shown in Fig. 3. An endothermic peak due to the melt of solid silybin with a peak top at 435.2 K is found. And an exothermic peak due to the decomposition of silybin with a peak top at 540.4 K is found.

Based on these observations, to measure the heat capacity for mixtures of silybin + PVP K30 by DSC, the temperature program should be operated below 406 K to avoid molecular decomposition, and the effect of water evaporation should be taken into consideration.

In this experiment, all samples were dried under vacuum at 333 K for 48 h before DSC test. However, during the process of sample be weighed and be loaded into crucibles, moisture will be absorbed by samples because of the hygroscopicity of solids. Within

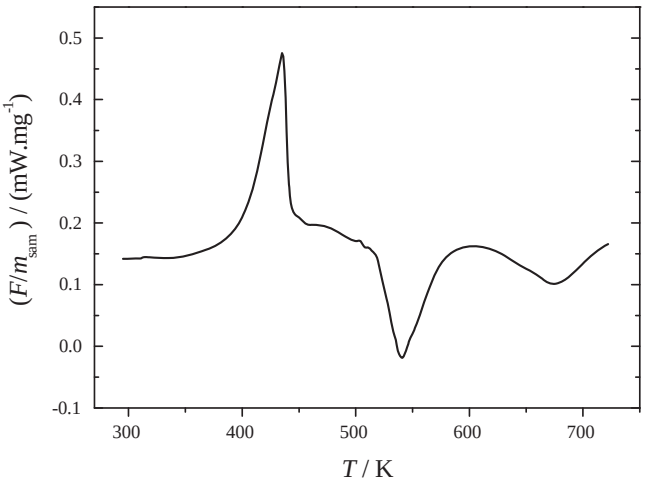

Fig. 3. The DSC curve of silybin.

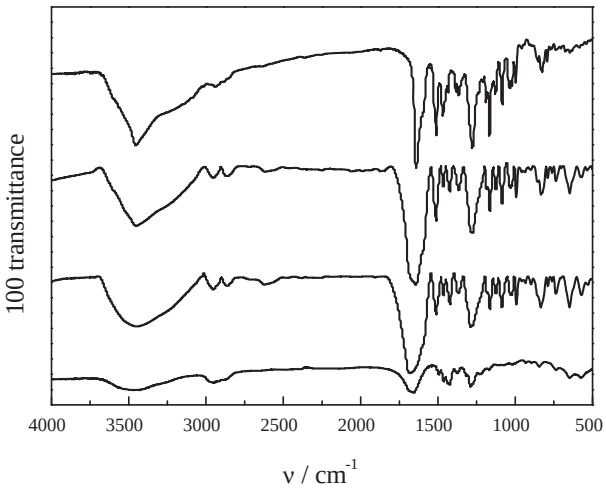

Fig. 5. FT-IR spectra (transmittance vs. wavenumber ν) of mixtures of [silybin(1) + PVP K30 (2)] with mass fractions of w_1 = 1, 0.5996, 0.3989, and 0 (in order from top to bottom).

the interval after the sample was loaded into the DSC instrument and before the C_p has been measured, DSC scan was performed under the protection of nitrogen gas to remove the water in sample. In Fig. 4, it shows the DSC scan was repeated four times for pure PVP K30. In which, a broad endothermic peak due to water evaporation below 393 K is found. Repeated scan leads the water peak to be depressed. In Fig. 4, the first two scans were F_{sam}/m_{sam}, where they were run to remove water. The third and fourth scans were $(F_{sam} - F_{bsl})/m_{sam}$, where they were recorded to evaluate the heat capacity, which is overlapped as expected. For silybin, the water removing by DSC scan is more easier than it does for PVP K30.

3.2. FT-IR spectroscopy

Infrared spectra were recorded in order to tell us if there were possible interactions and chemical reactions between silybin and PVP K30 in the solid state. The infrared spectra of silybin, PVP K30, and some of their mixtures (w_1 = 0.5996 and 0.3989), are shown in Fig. 5.

For silybin the band at 3450 cm^{-1} is assigned to free –OH bond vibration, 2900 cm^{-1} is assigned to the stretching vibration of C–H, 1640 cm^{-1} is assigned to the stretching vibration of the band of C=O group, 1500 cm^{-1} is assigned to aromatic group; 1270 cm^{-1} is assigned to =C–O–C vibration, 820 cm^{-1} is assigned to C–H of aromatic group bending vibration [18].

The spectrum of PVP K30 shows, among others, important band at 2950 cm^{-1} (C–H stretch), 1660 cm^{-1} (C=O) and 1280 cm^{-1}(C–N). A very broad band was also visible at 3450 cm^{-1} that was attributed to the presence of water confirming the broad endothermic peak detected in the DSC scan.

The peak corresponding to the C=O stretch of the amide function of PVP, is being shifted towards higher wave number for sample with w_1 = 0.3989. It changes from 1660 cm^{-1} for pure PVP, to 1679 cm^{-1} for the mixture of w_1 = 0.3989. The reason of this observation can be interpreted as a consequence of solid dispersion, where the hydrogen bonding between OH and C=O of silybin was replaced by the interaction between silybin and PVP. But for pure silybin and the sample of w_1 = 0.5996, the peak corresponding to the C=O stretch is 1640 cm^{-1}. Band shift was not observed. It may be attributed to the excess amount of silybin, which was unable to be dispersed into the solid dispersions. Furthermore, the broad band at 3540 cm^{-1} caused by H-bonding of water present in the samples, increases in intensity as the amount of polymer increases. These observations indicate that, with the increases in silybin, there is less amount of water present in these mixtures [8].

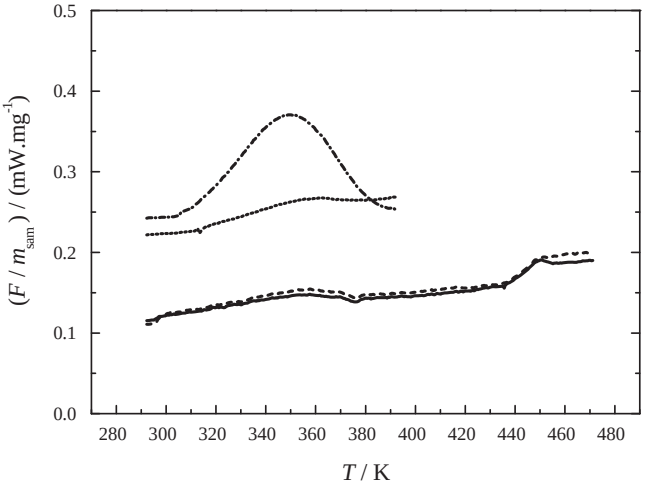

Fig. 4. DSC curves of four repeated scans to pure PVP K30. The first (dash dot line) and second (short dash line) scans (F_{sam}/m_{sam}) were run to evaporate water. The third (dash line) and fourth (solid line) scans [$(F_{sam} - F_{bsl})/m_{sam}$] were recorded to evaluate the heat capacity.

3.3. Heat capacity

The specific heat capacity C_p for samples of [silybin (1) + PVP K30 (2)] were measured at temperature ranging from 298.15 to 370.15 K by DSC. Binary samples with a mass fraction w_1, from 0.1 to 0.9 were prepared by the method of preparing solid dispersions. To eliminate the influence of water, the DSC scan was run repeatedly three times from ambient temperature to 373.2 K, and then C_p was measured during the fourth run.

The value of the composition (w_1) is determined in the process of preparing binary mixture as described in Section 2.2. During those processes of sample be weighed and be loaded into the DSC crucible, moisture absorption by sample is unavoidable. Therefore, we have three DSC scans under nitrogen protection to remove water. In the fourth scan, the mass loss was not observable. This has been confirmed by checking the weight of samples before and after the fourth run. The final mass after C_p test was chosen to calculate the heat capacity. Over the processes of DSC operation, the mass ratio of silybin to PVP was not changed. Only water and solvent were

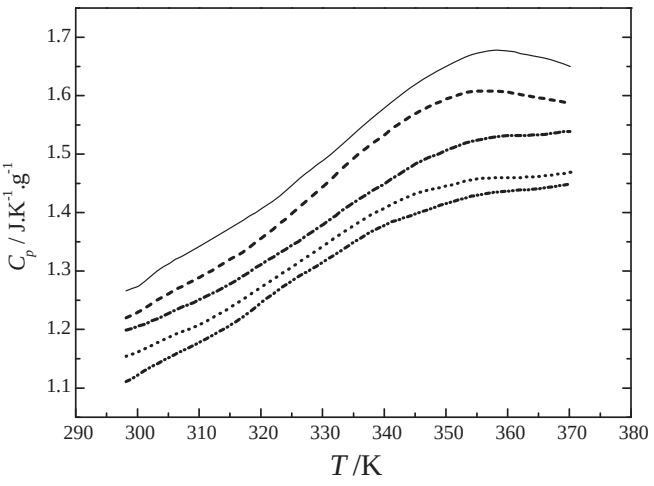

Fig. 6. C_p curves against temperature T/K for [silybin (1) + PVP K30 (2)] with mass fractions of w_1 = 0, (solid line); 0.1000, (dash line); 0.1994, (dash dot line); 0.2999, (dot line); 0.3989, (dash dot dot) by DSC.

absorbed and then be evaporated. Therefore, the initial value of the composition determined in Section 2.2 is still a better choice.

The C_p data are listed in the Table in Supplementary data. The C_p curves can be classified into two types according to their curve features. One is the curves of the solid dispersions with the shape similar to that of pure PVP K30. Another is the curves with the character of mixing solid dispersion and crystalline silybin. Figs. 6 and 7 show these two types of curves, respectively.

3.4. Equations to fit the C_p

There are many empirical equations to correlate the data of C_p with temperature and compositions [14–17]. For example, the dependence of C_p on temperature can be expressed by Eq. (2) in the range from an initial temperature T_i to a final temperature T_f.

$$C_p = a_1 + a_2x + a_3x^2 + a_4x^3 + a_5x^4 \quad (2)$$

where,

$$x = \frac{T - T_i}{T_f - T_i} \quad (3)$$

The coefficients of Eq. (2) can be obtained by fitting experimental data of C_p. For samples with w_1 = 0–0.4, the best form of Eq. (2) have four terms, that is from a_1 to a_4, and a linear relationship between a_i and w_1 is found.

$$a_i = a_{i1} + a_{i2}w_1 \quad (4)$$

The coefficients of Eq. (4) for samples of this group are listed in Table 1.

For samples of another group with w_1 = 0.5–1, the best form of Eq. (2) have five terms, a_1 to a_5. The values of a_i are listed in Table 1.

Equations of C_p against T are different for two groups of samples. Correspondingly, samples are in two different mixing states.

Table 1
The coefficients of Eq. (2) (a_i) and Eq. (4) (a_{i1} and a_{i2}) obtained by fitting C_p data in temperature range from 298.15 to 370.15 K, and the standard error s and the correlation coefficient R of the fit.

w_1 (range from 0 to 0.4)	
a_{11}	1.279
a_{21}	0.0962
a_{31}	1.334
a_{41}	−1.071
a_{12}	−0.4206
a_{22}	0.6164
a_{32}	−2.371
a_{42}	1.625

	w_1					
	0.5000	0.5996	0.6997	0.8001	0.8996	1
a_1	1.166	1.163	1.156	1.148	1.168	1.162
a_2	0.1504	0.5289	0.6805	0.7809	0.4882	0.5823
a_3	2.065	0.8688	0.4159	−0.3301	−0.1319	−0.9706
a_4	−3.663	−2.594	−2.268	−0.9659	−0.4872	1.351
a_5	1.736	1.576	1.563	0.9410	0.5381	−0.4137

3.5. The differential curve of C_p

To find the difference appeared in curve feature of two groups of samples, the differential curves of (dC_p/dT) against T are plotted in Figs. 8 and 9 for samples of (silybin + PVP K30), respectively. Some characteristic parameters can be extracted from these curves.

Fig. 8 presents the differential curves for samples with w_1 = 0–0.5. Obviously, there is one maxima point for each composition. Both the values of the maxima point, $(dC_p/dT)_{max}$ and temperature T(max), decrease with the increase in w_1. Fig. 10 gives the depression of T(max) with w_1. However, for the curve of w_1 = 0.5, there are two extreme points, one maxima at

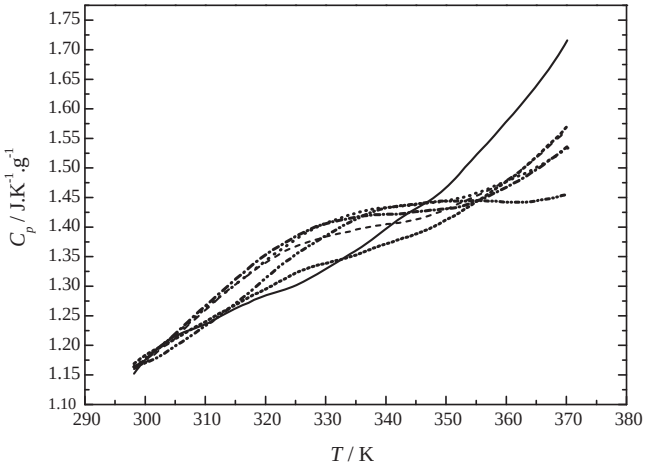

Fig. 7. C_p curves against temperature T/K for [silybin (1) + PVP K30 (2)] with mass fractions of w_1 = 0.5000, (dash dot dot line); 0.5996, (dot line); 0.6997, (dash dot line); 0.8001, (dash line); 0.8996, (short dash line) and 1.0 (solid line) by DSC.

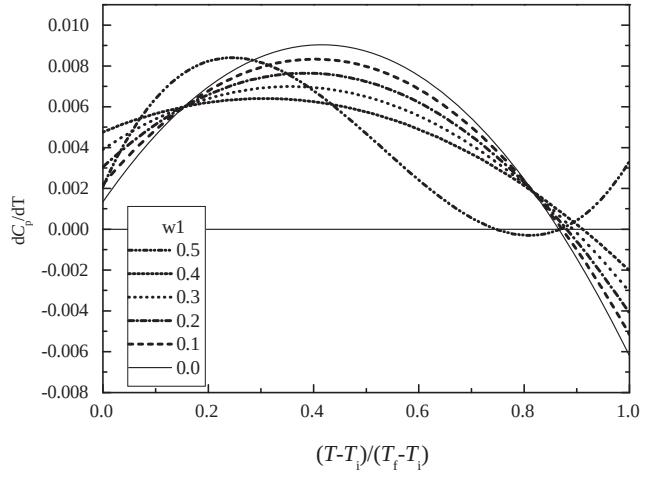

Fig. 8. The curves of (dC_p/dT) against $(T - T_i)/(T_f - T_i)$ for samples with mass fractions of w_1 = 0, (solid line); 0.1000, (dash line); 0.1994, (dash dot line); 0.2999, (dot line); 0.3989, (short dash line) and 0.5000 (dash dot dot line).

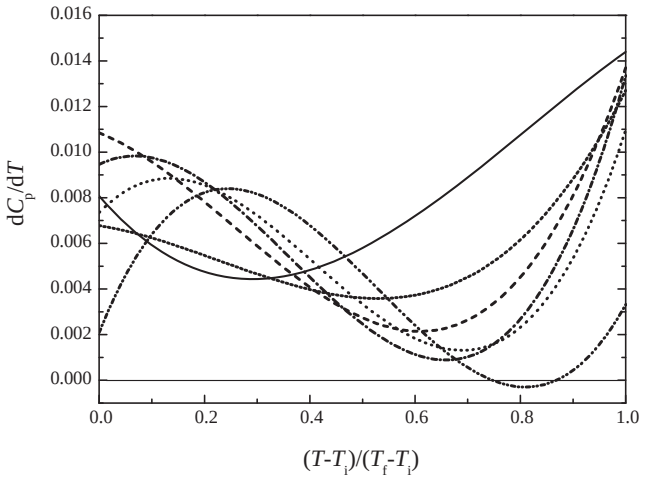

Fig. 9. The curves of (dC_p/dT) against $(T - T_i)/(T_f - T_i)$ for silybin + PVP K30 samples with mass fractions of $w_1 = 0.5000$, (dash dot dot line); 0.5996, (dot line); 0.6997, (dash dot line); 0.8001, (dash line); 0.8996, (short dash line) and 1.0 (solid line) by DSC.

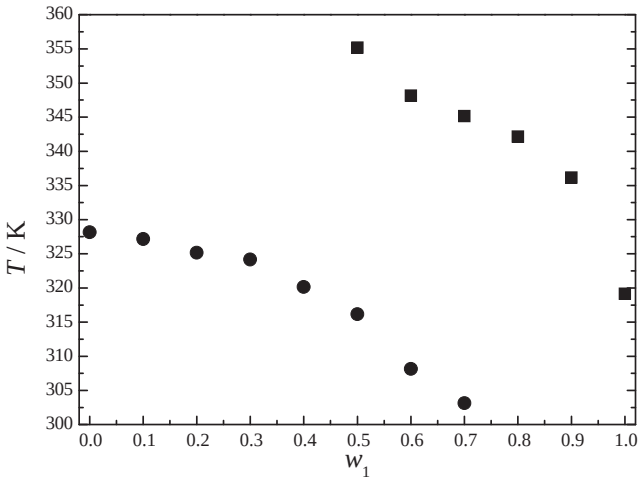

Fig. 10. The dependence of T(max) (●) and T(min) (■) on w_1.

T(max) = 316.15 K and one minima at T(min) = 355.15 K. Apparently, the character of that curve ($w_1 = 0.5$) is different from those curves of $w_1 = 0$–0.4. Because the shape of the differential curve of samples of $w_1 = 0.1$–0.4 are similar to the curve of pure PVP K30 ($w_1 = 0$), then it can be concluded that these samples have the solid state similar to PVP. That is to say that, silybin has been dispersed into the amorphous solid of PVP K30. However, as w_1 excess to 0.4, dispersion reaches to a saturation state, and excess amount of silybin crystallized from the amorphous dispersions. Therefore, a minima point outside the PVP amorphous scope is found in the composition of $w_1 = 0.5$.

Fig. 9 presents the differential curves for samples with $w_1 = 0.5$–1.0. There are two extreme points for these samples. One maxima point corresponds to the amorphous solid dispersions of silybin in PVP K30, and another minima point corresponds to the crystalline silybin. With w_1 increases, T(max) decrease and disappears until $w_1 = 0.8$. Whereas, the minima, with a value of $(dC_p/dT)_{min}$ as a characteristic parameter of crystal silybin,

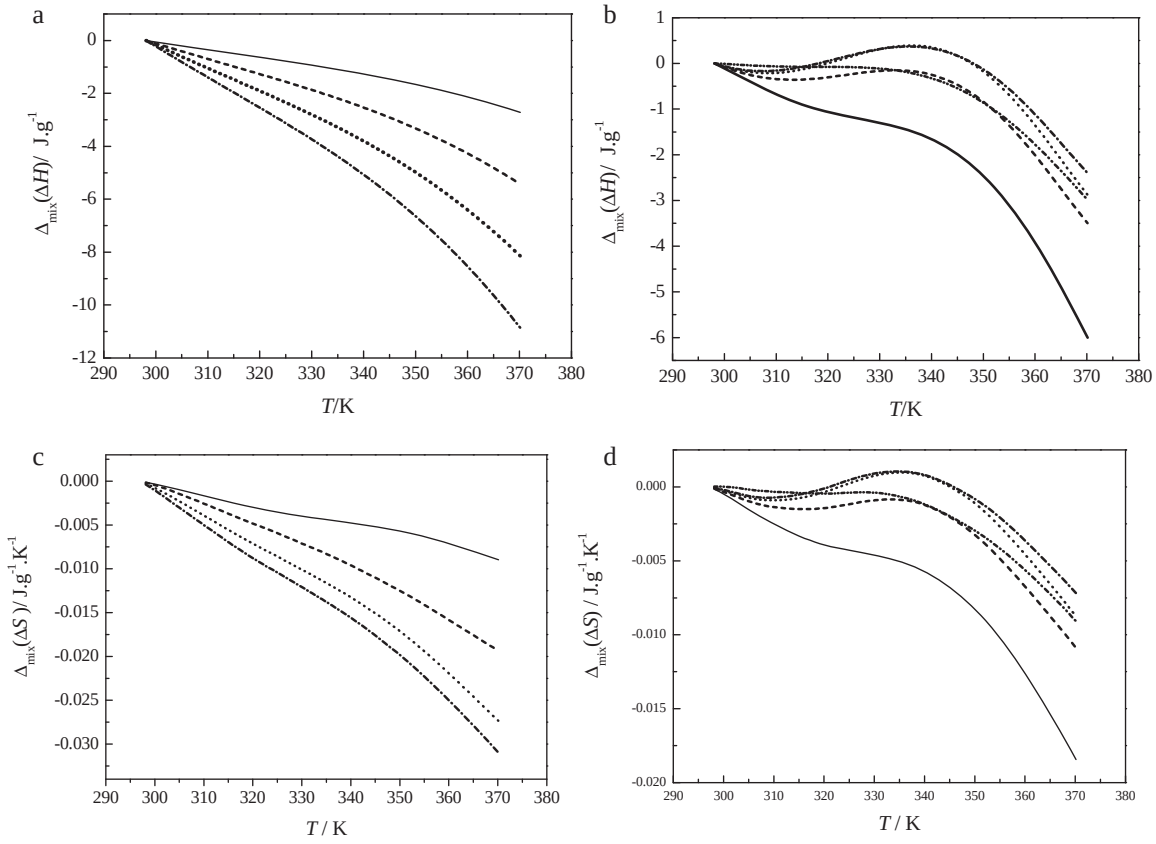

Fig. 11. The mixing thermodynamic properties of [silybin (1) + PVP K30 (2)] against temperature T. (a) Mixing enthalpy for mass fraction $w_1 = 0.1$, (solid line); 0.2, (dash line); 0.3, (dot line); and 0.4, (dash dot line); (b) mixing enthalpy for mass fraction $w_1 = 0.5$, (solid line); 0.6, (dash line); 0.7, (dot line); 0.8, (dash dot line), and 0.9 (dash dot dot line); (c) mixing entropy for mass fraction $w_1 = 0.1$, (solid line); 0.2, (dash line); 0.3, (dot line); and 0.4, (dash dot line); and (d) mixing entropy for mass fraction $w_1 = 0.5$, (solid line); 0.6, (dash line); 0.7, (dot line); 0.8, (dash dot line), and 0.9 (dash dot dot line).

Table 2
The temperature of the minima, T(min); the maxima, T(max); and the values of $(dC_p/dT)_{min}$ at the minima, and the $(dC_p/dT)_{max}$ at the maxima for curves of dC_p/dT against T for system of silybin + PVP K30.

w_1	T(min) (K)	$(dC_p/dT)_{min}$ (J g^{-1})	T(max) (K)	$(dC_p/dT)_{max}$ (J g^{-1})
1	319.15	0.00443		
0.8996	336.15	0.00358		
0.8001	342.15	0.00214		
0.6997	345.15	0.00088	303.15	0.00983
0.5996	348.15	0.00131	308.15	0.00885
0.5000	355.15	−0.00030	316.15	0.00840
0.3989			320.15	0.00640
0.2999			324.15	0.00699
0.1994			325.15	0.00764
0.1000			327.15	0.00833
0			328.15	0.00904

increases from w_1 = 0.5–1. Another characteristic parameter, the temperature of the minima T(min), decreases with w_1 increase. For w_1 < 0.4, the minima disappeared, which indicates silybin has been dispersed completely into the amorphous solid dispersion of PVP. The values of T(min) and T(max) are shown in Fig. 10. Parameters of extreme points, T(min), $(dC_p/dT)_{min}$, T(max), and $(dC_p/dT)_{max}$, are listed in Table 2.

From above discussion, it can be concluded that, a solid dispersion of silybin in PVP is formed in the region of w_1 < 0.4. As w_1 > 0.4, a mixture of crystalline silybin and an amorphous solid dispersion is formed.

3.6. Thermodynamic properties

The change in thermodynamic properties, from the initial temperature T_i to a given temperature T, can be calculated from the C_p data. Thermodynamic relations are given as below.

$$\Delta H = \int_{T_i}^{T} C_p dT \tag{5}$$

$$\Delta S = \int_{T_i}^{T} \frac{C_p}{T} dT \tag{6}$$

$$\Delta G = \Delta H - T\Delta S \tag{7}$$

Where, H, S and G are the enthalpy, entropy and Gibbs function, respectively. To evaluate the mixing effect, a mixing function, for example the mixing enthalpy, is defined by Eq. (8).

$$\Delta_{mix}\Delta H = \Delta H - (w_1\Delta H_1 + w_2\Delta H_2) \tag{8}$$

Where, ΔH, ΔH_1 and ΔH_2 are the enthalpy change defined by Eq. (5) for mixtures, pure component 1 (silybin) and 2 (PVP), respectively. The mixing enthalpy ($\Delta_{mix}\Delta H$) and entropy ($\Delta_{mix}\Delta S$) are graphically shown in Fig. 11. It can be found in the region of w_1 < 0.4 that, the mixing enthalpy ($\Delta_{mix}\Delta H$, Fig. 11a) and entropy ($\Delta_{mix}\Delta S$, Fig. 11c) are negative, and depress with the increase in both temperature and w_1. Whereas, in the region of w_1 > 0.4, the change of $\Delta_{mix}\Delta H$ and $\Delta_{mix}\Delta S$ (Fig. 11b and d) with T and w_1 is more complex. Some of them are negative, decrease with temperature raise, and increase with w_1 increase. For the cases of w_1 close to 1, the effect mixing is small.

4. Conclusion

The heat capacity C_p of solid mixture [silybin (1) + PVP K30 (2)] is an essential piece of data in predicting the thermodynamic properties and the phase state. It is valuable in the evaluation of the efficiency of drugs. From the differential curve of (dC_p/dT) against T, some apparent parameters, a maxima point and a minima point, characterizing the C_p curve and solid state have been obtained. The maxima point in the region of w_1 < 0.4 is a character of amorphous solid state of PVP. A solid dispersion of silybin in PVP is formed in this region. The minima point in the region of w_1 > 0.4 is a character of crystalline silybin, where a mixture of crystalline silybin and an amorphous solid dispersion is formed.

Appendix A. Supplementary data

Supplementary data associated with this article can be found, in the online version, at doi:10.1016/j.tca.2011.03.022.

References

[1] K. Flora, M. Hahn, H. Rosen, K. Benner, Milk thistle (*Silybum marianum*) for the theraply of liver disease, Am. J. Gastroenterol. 93 (1998) 139–143.
[2] N. Škottová, V. Krečman, Silymarin as a potential hypocholesterolaemic drug, Physiol. Res. 47 (1998) 1–7.
[3] D.Y.W. Lee, Y. Liu, Molecular structure and stereochemistry of silybin A, silybin B, isosilybin A, and isosilybin B, isolated from *Silybum marianum* (milk thistle), J. Nat. Prod. 66 (2003) 1171–1174.
[4] M.S. El-Samaligy, N.N. Afifi, E.A. Mahmoud, Increasing bioavailability of silymarin using a buccal liposomal delivery system: preparation and experimental design investigation, Int. J. Pharm. 308 (2006) 140–148.
[5] W. Han, T.C. Bai, J.J. Zhu, Thermodynamic properties for the solid–liquid phase transition of Silybin + Poloxamer 188, J. Chem. Eng. Data 54 (2009) 1889–1893.
[6] T. Vasconcelos, B. Sarmento, P. Costa, Solid dispersions as strategy to improve oral bioavailability of poor water soluble drugs, Drug Discov. Today 12 (2007) 1068–1075.
[7] S. Hasegawa, N. Furuyama, S. Yada, T. Hamaura, A. Kusai, E. Yonemochi, K. Terada, Effect of physical properties of troglitazone crystal on the molecular interaction with PVP during heating, Int. J. Pharm. 336 (2007) 82–89.
[8] I. Weuts, D. Kempen, A. Decorte, G. Verreck, J. Peeters, M. Brewster, G. Van den Mooter, Phase behaviour analysis of solid dispersions of loperamide and two structurally related compounds with the polymers PVP-K30 and PVP-VA64, Eur. J. Pharm. Sci. 22 (2004) 375–385.
[9] W.W. Yao, T.C. Bai, J.P. Sun, C.W. Zhu, J. Hu, H.L. Zhang, Thermodynamic properties for the system of silybin and poly(ethylene glycol) 6000, Thermochim. Acta 437 (2005) 17–20.
[10] J. Zhu, Z.G. Yang, X.M. Chen, J.B. Sun, G. Awuti, X. Zhang, Q. Zhang, Preparation and physicochemical characterization of solid dispersion of quercetin and polyvinylpyrrolidone, J. Chin. Pharmaceut. Sci. 16 (2007) 51–56.
[11] G. Van den Mooter, P. Augustijns, N. Blaton, R. Kinget, Physico-chemical characterization of solid dispersions of temazepam with polyethylene glycol 6000 and PVP K30, Int. J. Pharm. 164 (1998) 67–80.
[12] S. Sethia, E. Squillante, Solid dispersion of carbamazepine in PVP K30 by conventional solvent evaporation and supercritical methods, Int. J. Pharm. 272 (2004) 1–10.
[13] Z.H. Liu, Introduction to Thermal Analysis, Chemical Industry Press, Beijing, 1991.
[14] X. Hua, D. Kaplan, P. Cebe, Effect of water on the thermal properties of silk fibroin, Thermochim. Acta 461 (2007) 137–144.
[15] K. Xu, J. Song, F. Zhao, H. Ma, H. Gao, C. Chang, Y. Ren, R. Hu, Thermal behavior, specific heat capacity and adiabatic time-to-explosion of G(FOX-7), J. Hazard. Mater. 158 (2008) 333–339.
[16] B. Tong, Z.C. Tan, Q. Shi, Y.S. Li, D.T. Yue, S.X. Wang, Thermodynamic investigation of several natural polyols (I): heat capacities and thermodynamic properties of xylitol, Thermochim. Acta 457 (2007) 20–26.
[17] M. Mundhwa, S. Elmahmudi, Y. Maham, A. Henni, Molar heat capacity of aqueous sulfolane 4-formylmorpholine, 1-methyl-2-pyrrolidinone, and triethylene glycol dimethyl ether solutions from (303.15 to 353.15) K, J. Chem. Eng. Data 54 (2009) 2895–2901.
[18] J.X. Xie, J.B. Chang, X.M. Wang, Infrared Spectroscopy Application in Organic Chemistry and Drug Chemistry, Science Press, Beijing, 2001.